Temperature, Surface, and Coverage-Induced Conformational Changes of Azobenzene Derivatives on Cu(001)

M. Piantek,*,† J. Miguel,† A. Krüger,† C. Navío,† M. Bernien,† D. K. Ball,† K. Hermann,‡ and W. Kuch†

Institut für Experimentalphysik, Freie Universität Berlin, Arnimallee 14, 14195 Berlin, Germany, and Fritz-Haber-Institut der Max-Planck-Gesellschaft, Faraday-Weg 4-6, 14195 Berlin, Germany

Received: August 7, 2009; Revised Manuscript Received: October 9, 2009

The adsorption of dimetacyano azobenzene (DMC) and carboxymethylester azobenzene on metallic surfaces has been studied by means of X-ray photoelectron spectroscopy, near-edge X-ray absorption fine structure, and density functional theory (DFT) calculations. We find that the molecule coverage and chemical character of the substrate and its temperature have an influence on the adsorption state. On a Au(111) substrate at room temperature, DMC physisorbs flat in its trans configuration up to a saturation coverage of one monolayer, while the electronic structure of the adsorbate resembles the one calculated for the free molecule. In a submonolayer evaporated on Cu(001) at 150 K, the majority of DMC molecules is found to be in the same physisorbed state as on Au(111). After annealing the substrate above 250 K most of the molecules chemisorb via their azobenzene center, where N−Cu bonds are formed, while the central azo N═N double bond is weakened. The attractive forces between the center of the molecule and the surface, together with a repulsive phenyl−metal interaction, lead to a butterfly-like bent molecular geometry in which the outer aromatic groups are tilted out of the surface plane. At higher coverages, the increased intermolecular interaction provokes a stronger tilt that finally leads to a cleavage of the central N═N azo double bond.

Introduction

The utilization of controllable reversible processes in molecules on surfaces discloses a completely new path into miniaturization. For instance, the photon-triggered transition between two different isomers offers the possibility to switch between two states that exhibit strikingly different physical and chemical properties. In particular, azobenzene molecules in gas phase and solution undergo such photoisomerization, where the transformation is concomitant with conformal changes in the chemical structure. This behavior makes them suitable for the development of, for example, molecular motors,[1] or for the mechanical manipulation of secondary molecules.[2] Conversely, such applications bring the molecular switch into a confinement, where the isomerization process is strongly influenced, not only by mechanical coupling but also by electronic interaction of the molecule with the environment.

Several attempts have been made to prepare surfaces with functionalities of photosensitive systems in order to control the surface properties. Recently, the realization of a photoswitchable ensemble of azobenzene molecules fixed via linker/spacer groups to a glass surface has been successfully demonstrated.[3] Obviously, the direct adsorption of conformal switches on a surface can be rather complex. In contrast to gas phase and solution, the degree of freedom is reduced due to adsorbate−adsorbate[4] and adsorbate−surface interactions.[5,6] The presence of the latter has been demonstrated by using a scanning tunneling microscope (STM) tip to switch a single trans azobenzene molecule on a Cu(001) surface at 5 K, where the resulting cis isomer was stabilized by chemisorption to the substrate, preventing the reverse transformation.[6] It was further shown that the adsorption of one monolayer azobenzene on Cu(001) at room temperature leads to a more cis-like adsorption geometry[7] while for the same temperature the trans conformation is preferred on an inert Au(111) surface. This suggests that substrate reactivity can be used to tune the switching process to allow reversibility.[8] Furthermore, the interplay of adsorbate−substrate and adsorbate−adsorbate interactions with the molecular bistability could be used, for example, in bottom-up epitaxy.

While most of the related research on azobenzene derivatives adsorbed at metallic surfaces has been performed by STM,[4–6,9–11] the present study provides complementary information that leads to a more detailed picture of the involved adsorption mechanisms. Here angle-dependent near edge X-ray absorption fine structure (NEXAFS) is used to study the adsorption geometry, while both NEXAFS and X-ray photo electron spectroscopy (XPS) yield information concerning the electronic properties of the adsorbed molecules. In addition, a detailed interpretation of the experimental NEXAFS data requires strong theoretical support which is provided in the present study by model spectra based on density functional theory (DFT) calculations. Dimetacyano azobenzene (DMC), as shown later in Figure 1a, is used as an azobenzene model system, since the C≡N cyano rest groups exhibit a crossed π-orbital system that can be used to get more detailed information about the molecular orientation from the angle dependence of the cyano N-*K* edge NEXAFS.[12] Since for DMC the nitrogen-*K* edge NEXAFS and the N 1s XPS contain the convoluted contributions of both, the central azo nitrogen and the cyano rest group, dimetacarboxymethylester azobenzene (CMA) with the geometric structure given in Figure 1b, is used as a reference system since here the nitrogen core excitation processes only originate from the center of the molecule. To study the effect of different adsorbate−substrate interactions, the adsorption on the more inert Au(111) surface

* To whom correspondence should be addressed. E-mail: piantek@physik.fu-berlin.de.
† Freie Universität Berlin.
‡ Fritz-Haber-Institut der Max-Planck-Gesellschaft.

10.1021/jp907641f CCC: $40.75
Published on Web 10/28/2009

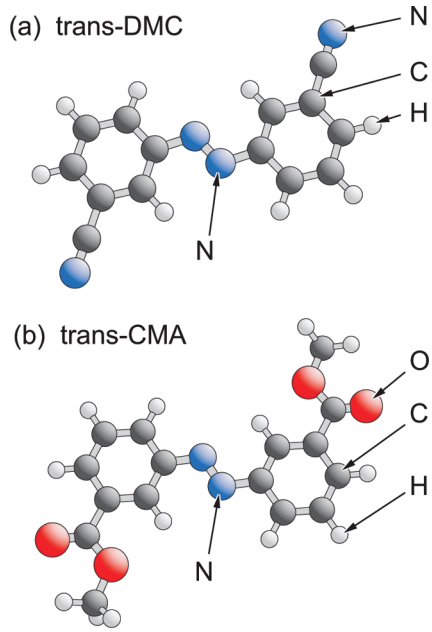

Figure 1. Geometric structures of (a) DMC and (b) CMA. For the latter, the central NN azo bridge connects two benzonitrile moieties. The color of the balls is assigned to the element as follows: black, carbon; white, hydrogen; blue, nitrogen; and red, oxygen.

is compared with the one on the more reactive Cu(001) surface. For the latter a transition from the physisorbed to the chemisorbed state is followed by means of temperature-dependent XPS and NEXAFS. For chemisorbed DMC molecules on Cu(001) at room temperature the influence of the intermolecular interactions on the adsorption state is demonstrated by coverage-dependent NEXAFS and interpreted with the help of DFT calculations.

Experimental Section

All experiments were performed in an ultrahigh vacuum system with a base pressure of 10^{-8} Pa equipped with standard surface science tools. The Au(111) and Cu(001) substrates were cleaned by repeated cycles of Ar^+ ion sputtering at 800 eV and 1 keV, respectively, and subsequent annealing to 900 K until sharp low energy electron diffraction spots appeared, and no contamination of the surface could be detected by XPS.

DMC and CMA have been synthesized by Professor K. Rück-Braun and co-workers at the Technische Universität in Berlin. Monolayer and submonolayer coverages of molecules were prepared by evaporation from a Knudsen cell at 350−380 K onto the clean metallic substrates. The deposition on Au(111) and Cu(001) at room temperature saturates at a maximum coverage. For the Au(111) substrate, we refer to this coverage as 1 monolayer (ML) of molecules. For Cu(001), this saturation coverage is found to be 1.3 ML as it will be explained in detail later in the text.

X-ray absorption spectra were taken using synchrotron radiation from the undulator beamline UE56/2-PGM2 of BESSY in Berlin. Linearly p-polarized light with a degree of polarization ≥90% was used. The incidence angle was varied between 20 and 90° with respect to the surface plane. Absorption spectra were acquired in total electron yield mode recording the sample drain current as a function of photon energy. Beam intensities were monitored by the photon yield from a freshly evaporated gold grid. The photon energy resolution was set to 130 meV. To minimize the effects of radiation damage, the photon intensity was reduced using higher constant fixed focus values of the monochromator. The estimated typical photon flux density at the sample was about 10^{13} s^{-1} cm^{-2}. From the comparison of spectra taken immediately after preparation of the sample and at later times we conclude that radiation damage can be excluded for the measurements presented here.

XPS measurements were performed using a SPECS Phoibos 100 electron analyzer at a typical energy resolution of 600 meV with 20 eV pass energy. The dipole beamline PM3 and the undulator beamline UE56/2 PGM2 at BESSY have been used as light sources. The excitation energy was 500 eV with a photon energy resolution of 300 meV. Binding energies have been calibrated at the Au $4f_{7/2}$ binding energy at 84.0 eV. The electron takeoff angle was set to 90° corresponding to normal emission while the incidence angle of the p-polarized X-rays was 45°.

Calculations

Quantum chemical calculations using the StoBe code[13] were performed in order to obtain theoretical angle-resolved NEXAFS spectra. The calculations are based on density functional theory (DFT) in combination with gradient-corrected exchange/correlation functionals due to Perdew, Burke, and Ernzerhof (RPBE)[14,15] and Gaussian basis sets to represent ground states as well as final states for carbon and nitrogen core electron excitations. All-electron triple-ζ valence plus polarization (TZVP) basis sets are applied for carbon and nitrogen,[16] while a smaller basis set (double-ζ plus polarization) is used for hydrogen to evaluate electronic ground states. The calculations of the core excited states are carried out using a basis set of all-electron individual gauge for localized orbitals (IGLO-III) quality[17] to represent the excitation center, while the remaining equivalent atomic centers are described by effective core potentials (ECP)[18] approximating the 1s core and corresponding valence basis sets. In addition, a large diffuse even-tempered [19s,19p,19d] basis set was included at the excitation center in order to comprise the unbound states in the core region of the excited atom.[19]

As an initial procedure for all NEXAFS calculations geometry optimizations are performed on the corresonding model systems. For the free trans DMC molecules and the trans DMC molecules on a Cu_{68} (001) cluster literature values are used as an input for the initial coordinates.[20,21] The final calculated geometry parameters are found to deviate by less than 5% from the published data. In the case of dissociated DMC on Cu(001), top, hollow, and bridge adsorption sites are used as initial geometries, all leading to the hollow site configuration.

The subsequent calculations of the N-*K* edge NEXAFS spectra are carried out using Slater's transition state (TS) method,[22,23] where transition energies are corrected by adjusting corresponding ionization potentials (IP) evaluated with the TS method at their values of fully relaxed ΔKohn−Sham DFT calculations. The discrete excitation spectrum obtained by the calculations is processed by a Gaussian convolution of energy-dependent broadening in order to compare the theoretical results with those of the experiment. For transitions below the ionization barrier a full width at half-maximum (fwhm) of 0.7 eV was applied, while the fwhm was increased linearly up to 4.5 at 10 eV above the IP. Further details of the methods are described in refs 24 and 25.

Results and Discussion

Physisorption on Au(111). In Figure 1, the geometric structures of the symmetrically functionalized azobenzenes CMA and DMC are shown. In both cases the central N═N azo

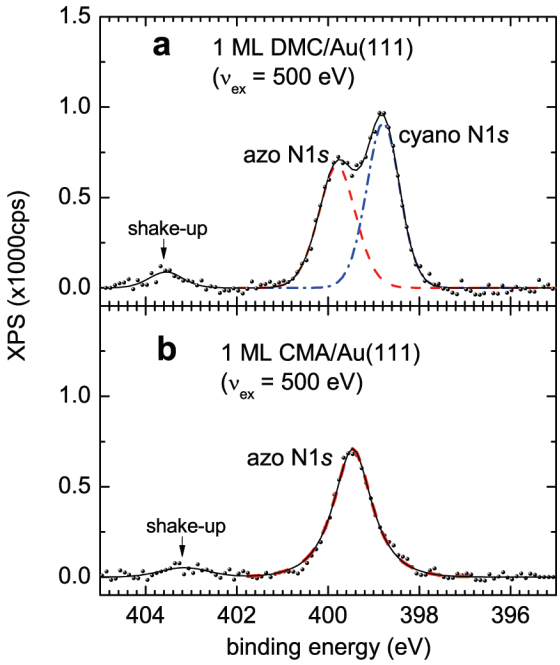

Figure 2. XP spectra of 1 ML of (a) DMC, and (b) CMA molecules evaporated on Au(111) at room temperature. Peak energies are calibrated to the Au $4f_{7/2}$ XPS signal at 84.0 eV. The dashed red and the dashed-dotted blue lines are the fitted curves for the azo and cyano excitation centers, respectively.

bridge connects two benzene rings that are equally substituted at the meta positions. For DMC, the aromatic side groups are benzonitril units whereas for CMA they are methyl benzoate.

Figure 2a shows the N 1s photoemission spectrum of 1 ML DMC on Au(111). Two strong peaks at 398.8 and 399.8 eV, originating from the two nonequivalent N 1s excitation centers in the azo bridge and the cyano rest group, are visible. The cyano groups exhibit a strong permanent dipole moment with an increased electron density at the nitrogen site.[26] Their electron-accepting character pulls the negative charge toward the rest groups of the molecule. As a result, the central azo group is expected to carry less negative charge in the initial ground state of the molecule. This leads to a chemical shift such that the azo N 1s XPS exhibits a higher binding energy than the one of the negatively charged cyano N 1s excitation center. Additionally, a higher local electron density at the rest groups in the final state will increase the hole screening for the electrons emitted from the cyano core levels, so that the splitting of the measured core level binding energies of the azo and the cyano nitrogen centers are strengthened. As an additional support for this peak assignment, we present in Figure 2b the N 1s XP spectrum of 1 ML CMA on Au(111). The single peak at 399.5 eV results from the photoemission of the N 1s azo core electrons, since CMA contains nitrogen atoms only in the azo bridge. The slight difference in binding energies of the azo XPS peaks of DMC and CMA can be explained by the lower electron affinity of the ester rest groups compared to that of the cyano groups.[27]

Additional low intensity peaks are visible at higher energies of 403.6 and 403.1 eV for DMC and CMA, respectively. For monosubstituted benzene, it has been shown that such shakeup intensities can be observed if the main ionization transition is coupled to an additional electronic $\pi \rightarrow \pi^*$ excitation.[28] In the case of DMC, the smaller intensity of the azo-N 1*s* peak, compared to the one of the cyano nitrogen, indicates that the shakeup process is only coupled to the ionization at the azo center. This is consistent with the particularly weak mixing of the π systems of azobenzene and benzonitrile (see Figure 3). Hence we can assign the shakeup peak to a coupling between the azo-N 1*s*-photoemission process and the electronic transition from one of the highest occupied molecular orbitals (HOMOs) to one of the lowest unoccupied molecular orbitals (LUMOs) at the azobenzene center.

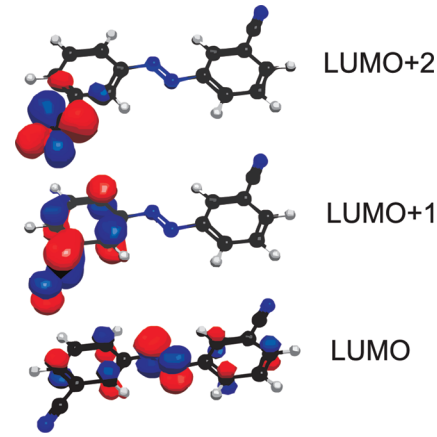

Figure 3. Selected LUMOs calculated by the transition state method for the free trans DMC.

In Figure 4a, angle-dependent N-*K* edge NEXAFS spectra are given for 1 ML DMC evaporated on Au(111) at 300 K, where the solid and dashed lines correspond to 90° normal and 20° grazing light incidence with respect to the metal surface, respectively. Two prominent resonance peaks in the range from 397 to 401 eV are caused by transitions from the N 1s core levels into the π^*-type lowest unoccupied molecular orbitals (LUMOs). From the angle dependence, we see that the peak at 399.7 eV, labeled as B and most prominent at normal incidence, corresponds to a transition to a π^*-orbital lying in the surface plane. A broader peak at 398.6 eV, labeled as A, dominates at grazing incidence and is attributed to transitions into a π system perpendicular to the surface. The opposite angular dependence of the transition intensities of these two peaks can be explained by studying the electronic structure of the molecule by means of DFT calculations.

In Figure 3, the three calculated LUMOs obtained from the transition state method are shown for a free planar trans DMC isomer. The LUMO is preferentially located at the azo center and perpendicular to the molecular plane, whereas the LUMO+1 and LUMO+2, concerning the triple C≡N bond in the benzonitrile moieties, are oriented out of plane and in plane, respectively. The localization of the LUMOs around the different N 1*s* excitation centers can be explained by considering the different orbital symmetries. Since the LUMO of the azobenzene has a node at the meta position it cannot couple to the LUMOs of the rest groups[29] and the π systems of azobenzene and benzonitrile can be regarded as independent. Thus, each orbital contributes only to one single resonance in the entire NEXAFS spectrum. Accordingly, the NEXAFS spectrum at lower energies comprises three π^* resonances that originate from electronic transitions into the three LUMOs. One resonance relates to the azobenzene N 1s → LUMO transition, while the rest groups contribute with two resonances as found for the NEXAFS of benzonitrile.[30,31] Identifying the molecular plane in the calculation with a hypothetical plane, we can simulate the angle-dependent NEXAFS spectra (see Figure 4b). Regarding the alignment of the transition state orbitals of Figure 3 with respect

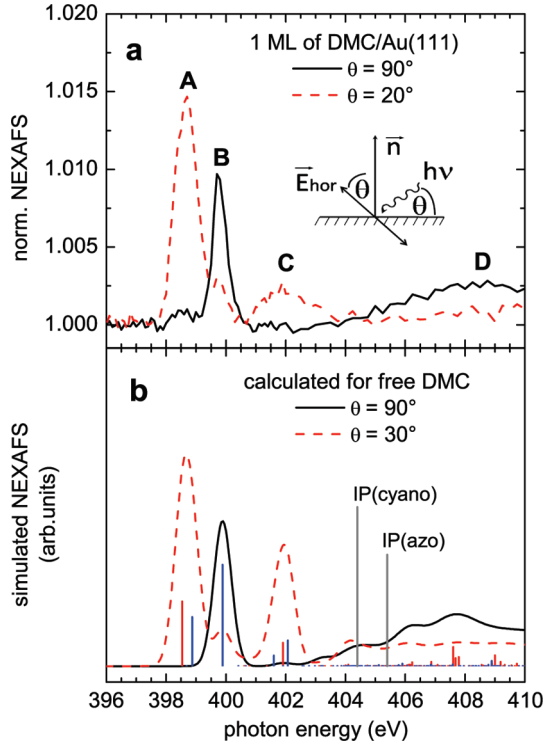

Figure 4. (a) Angle-dependent N-*K* edge absorption spectra of 1 ML of DMC molecules on Au(111). (b) Simulated NEXAFS spectra of a free trans DMC molecule. Solid (dashed) lines correspond to spectra at 90° normal (20 and 30° grazing, respectively) X-ray incidence. For the angular dependence of the calculated spectrum, the molecular plane corresponds to the surface plane in the inset in panel a. The transition dipole moments are presented below the calculated curves as vertical red and blue lines for the partial absorption of the azo and cyano excitation centers, respectively. The two gray vertical lines at 404.4 and 405.4 eV mark the ionization potentials of the cyano and the azo N 1s core levels, respectively.

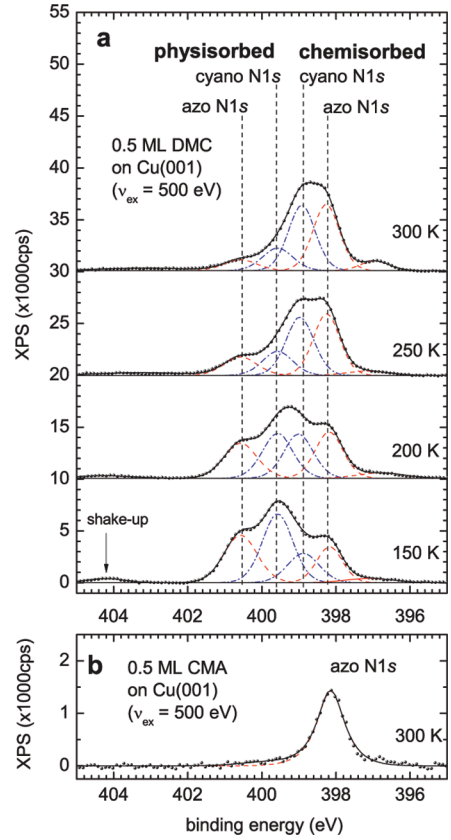

Figure 5. (a) Temperature-dependent N 1s XPS of 1 ML DMC molecules evaporated on Cu(001) at 150 K. Spectra are shifted vertically for clarity. (b) N 1s XPS signal from 1 ML CMA molecules evaporated on Cu(001) at 300 K. The dashed red and the dashed-dotted blue lines are the fitted curves for the azo and cyano excitation centers.

to this surface plane, the transitions into the out-of-plane LUMO and LUMO+1 are present as a broader peak A at grazing incidence, and the transition into the in-plane LUMO+2, as a narrower peak in the spectrum of normal incidence. The experimental data at grazing angle of 20° agrees best with the simulated curve for 30°. This may be explained by Fresnel diffraction that appears due to the interaction of the incoming X-ray wave with the electron density at the surface.[32] The quantitative agreement of the π^* resonances with those in the angle-dependent spectra of the adsorbed DMC molecules on Au(111) allows us to conclude that the molecule lies flat on the surface. Furthermore, the overall shape of the measured spectra is reproduced by the calculations, except for the overestimated intensity at 401.9 eV (peak C). This discrepancy is most likely due to the absence of the surface in the calculations.[33]

We can compare the calculated ionization potentials for the azo and cyano N 1s core electrons, 404.4 and 405.4 eV, respectively, with the corresponding binding energies derived from XPS (cf. Figure 2a). We find a perfect agreement in the order of the azo and cyano binding energies, as well as in their energy difference of 1.0 eV. The deviation in absolute energies is simply caused by the different references. The measured values are given with respect to the Fermi edge of the substrate, while the calculated ones are referenced to the vacuum level. The energy difference between the two references corresponds to the Au(111) work function.[34] We can thus conclude that 1 ML DMC physisorbs flat on Au(111) in the trans configuration at room temperature. Furthermore there is no indication for intermolecular coupling at the surface.

Temperature-Dependent Chemisorption on Cu(001). As a system with stronger molecule−substrate interaction, chemisorption of organic molecules on Cu(001) is quite likely to happen at room temperature. In contrast, for sufficiently low temperatures the thermal energy is not large enough to overcome the activation barrier for the chemical bond formation. Thus, we studied the temperature dependence of the adsorption state of DMC molecules in a temperature range between 150 K and room temperature. In Figure 5a, we show the N 1s XPS spectrum of 0.5 ML of DMC molecules evaporated on Cu(001) at 150 K for different substrate temperatures. At 150 K, four different peaks are needed to fit the main spectrum in the region between 397 and 402 eV. The relative distance of the two peaks at higher binding energies of around 1.0 eV is identical to the difference between the azo and the cyano N 1s binding energies found for physisorbed DMC molecules in the previous section. An additional weak shakeup resonance is present at 404.2 eV with a difference of 3.7 eV to the closest XPS peak. This value is identical to the one between the shakeup and the azo-N 1s peak for DMC physisorbed on Au(111). Thus we conclude that a substantial fraction of the molecules is physisorbed at the surface, which results in a perfect agreement of the XPS intensity above 399 eV with the corresponding spectrum for DMC on Au(111) (Figure 2a).

Two additional peaks, separated by 0.6 eV, are found at lower energies of 398.2 and 398.8 eV. A shift of the binding energies

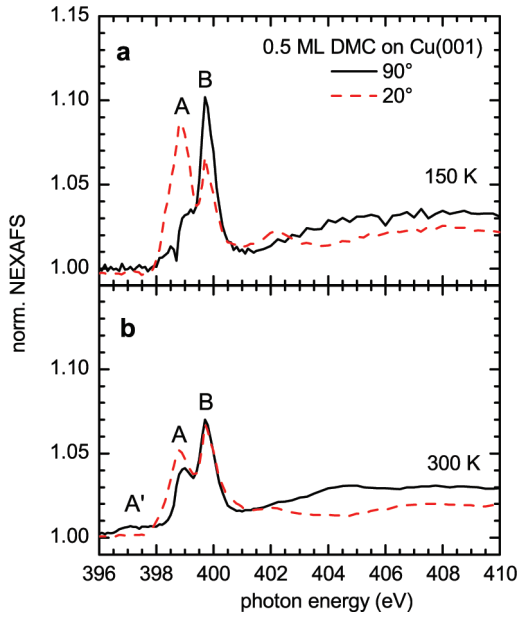

Figure 6. Temperature-dependent NEXAFS spectra of 0.5 ML DMC molecules evaporated on Cu(001) at 150 K (a) and after increasing the temperature to 300 K (b).

to lower values is generally expected to be caused by chemisorption at metallic substrates,[34] where electron donation from the substrate overcompensates the chemical shift of the azo center induced by the rest groups.[35] Thus, the same surface-induced chemical shift is expected for CMA. The N 1s XPS signal of 0.4 ML CMA evaporated on Cu(001) at room temperature (Figure 5b) shows an energy shift of 1.3 eV to lower binding energies compared to the one of CMA on Au(111), indicating chemisorption of the CMA molecules at Cu(001). Correspondingly, the peak of CMA on Cu(001) at 398.2 eV coincides in energy with the rightmost peak of DMC at 150 K, so that we can assign the peak at 398.2 eV to the azo N 1s core level ionization of DMC. As a result, a change in the order of the azo and the cyano N 1s signals appears. The comparison with physisorbed DMC thus suggests than that the rest groups are much less influenced by the effect of electron donation from the surface. We conclude that at 150 K there is a mixture of chemisorbed and physisorbed DMC molecules where the former are bound to the Cu(001) surface via their azo group.

At higher temperatures, the amount of the chemisorbed DMC increases at the expense of the physisorbed species according to the change in the peak ratio. The transformation is almost complete at 250 K, but a small amount of physisorbed DMC is still recognizable even at 300 K. This remnant of physisorbed molecules might exist probably because they cannot approach the surface appropriately in order to form a bond with the substrate. Furthermore, the shakeup resonance vanishes during the chemisorption process, indicating a change in the electronic structure at the azo center (compare with the previous section).

Obviously, the XPS data suggest a mixture of physisorbed and chemisorbed DMC molecules to be present on Cu(001) at 150 K. The corresponding NEXAFS spectra for 0.5 ML DMC molecules on Cu(001) at 150 K are shown in Figure 6a. The contribution of the physisorbed species can be assimilated to the one of DMC molecules on Au(111), so that differing features can be assigned to the chemisorbed phases. The different shapes observed for peak A at 398.7 eV for grazing and normal incidence geometries can be explained by considering that there are two contributing resonances (similar to the peak A in the spectrum of DMC on Au(111) in Figure 4a). At lower energies, the azo π^* orbital remains out of the surface plane, but the lower intensity of peak A with respect to the in-plane resonance at 399.7 eV, labeled as peak B, implies a weakening of the N═N double bond, caused by a bond formation with the metallic substrate.[36] In contrast, the shoulder at 398.9 eV in the normal incidence spectrum of the out-of-plane cyano orbital evidence that the benzonitrile moieties are tilted out of the surface plane. This results also in a modified angle dependence of peak B of the in-plane cyano orbital which can be explained by the formation of bonds with the metallic substrate that force the molecule to adopt a different orientation on the surface. In addition, the intermolecular interactions can have an influence on the orientation of the benzonitrile moieties.

The NEXAFS spectra at 300 K (Figure 6b) exhibit an enhancement of the characteristic features of the chemisorbed species. The absence of angle dependence of peak B can be explained by the fact that the majority of DMC molecules is chemisorbed, as evidenced by XPS, and all DMC molecules are either uniformly ordered with an angle of 35.3° between the in-plane orbital and the surface plane (magic angle for linearly polarized light), or completely disordered. However, the presence of a residual angle dependence of peak A favors the former scenario. The total cross section, which can be roughly estimated by adding the intensity of grazing and the double intensity at normal incidence, decreases for the peak B at 399.7 eV when going from 150 to 300 K. From the examination of the C 1s/Cu $3p_{3/2}$ XPS intensity ratios, it is seen that the amount of carbon and thus the molecular coverage does not change during annealing to room temperature. We therefore explain the higher total absorption intensity of peak B at 150 K by an additional contribution of the peak A which becomes much broader after annealing. By the discussed decrease in intensity of feature A during annealing the intensity of peak B appears smaller, although its total cross section may not change.

So far, we can conclude that DMC binds via its azo center to the Cu(001) surface. To elucidate whether the surface-molecule or the intermolecular interaction dominates, the conformational effect, we varied the molecular coverage at the surface as described in the next sections.

Adsorption Geometry at Low Coverage on Cu(001). To study the molecule-surface interaction individually, we evaporated 0.4 ML of CMA and DMC molecules on the Cu(001) surface at room temperature where it is likely that chemisorption takes place before the molecules can form islands. The corresponding NEXAFS spectra are shown in Figure 7a,b, respectively. For the physisorbed species of CMA molecules on Au(111), the NEXAFS spectrum exhibits only one sharp π^* resonance below the ionization barrier at 398.2 eV photon energy, as it was shown in ref 7. For a submonolayer on Cu(001) at room temperature, this π^* resonance is substituted by two broad resonances, as it can be seen in Figure 7a, attesting the weakening of the central azo π bond. The bond formation between the nitrogen atoms and the Cu(001) surface is also reflected by the broad spectral shape that can be assigned to the hybridization of the involved orbitals. From the angle dependence of these features it is evident that they remain oriented mainly perpendicular to the surface implying that the adsorbate−surface bonding character is σ-like. While the N-*K* edge NEXAFS spectra on Cu(001) prove the chemisorption of CMA, it was demonstrated in ref.[7] that the O-*K* edge does not show any substrate dependence indicating that the rest groups are not involved in the chemisorption process.

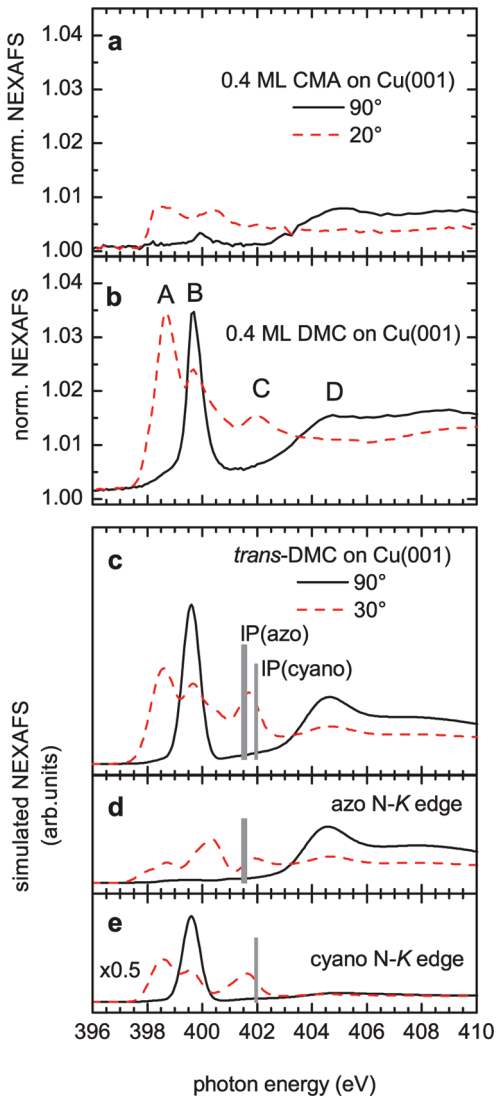

Figure 7. N-*K* edge NEXAFS spectra of 0.4 ML CMA (a) and DMC molecules (b) deposited on Cu(001) at room temperature. (c) Simulated NEXAFS spectra for a single DMC molecule on a Cu(001) cluster, in which the contributions of the azo (d) and the cyano (e) excitation centers are plotted individually. Gray bars mark the corresponding ionization barriers. Continuous lines correspond to spectra acquired or simulated for 90° normal X-ray incidence while dotted lines correspond to the spectra measured under 20° grazing and simulated for 30° grazing X-ray incidence.

In the case of DMC, the two nonequivalent nitrogen excitation centers contribute differently to the N-*K* edge NEXAFS spectra, which can be compared to the corresponding DFT calculations. The relaxed structure of a DMC molecule on a $Cu_{(38,\,30)}$ cluster (Figure 8) shows that the azo center is attracted to the two central Cu atoms, and that the outer parts are tilted by 9° with respect to the surface plane. This leads to a distortion of the crystalline Cu structure with atom displacements below 0.5 Å. In addition, the N═N bond is stretched from 1.287 to 1.339 Å by the attractive forces in the two N−Cu bonds. The simulated angle-dependent spectra of a single DMC molecule on the $Cu_{(38,\,30)}$ cluster (Figure 7c) resemble strikingly the experimental data of Figure 7b. The contributions of the azo and cyano N 1s excitation centers can be identified separately (panels d and e). Compared to the simulated spectra on Au(111), a clear change in the overall azo N-*K* edge spectra is evident, whereas the cyano contributions are rather unperturbed. Similar to the measured

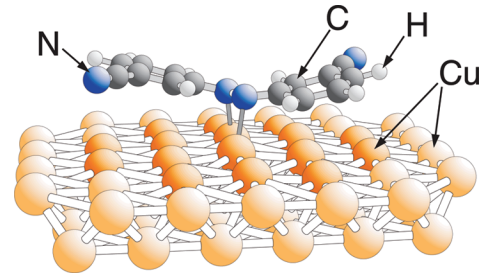

Figure 8. Relaxed geometric structure of a single DMC azobenzene molecule on top of a $Cu_{(38,\,30)}$ cluster, resulting from DFT geometry optimization. Darker and brighter substrate atoms were free and fixed during optimization, respectively.

spectra of CMA on Cu(001), the single π^* resonance of the DMC azo N-*K* edge splits into two broad features due to the hybridization of the azo π^* orbitals with the valence bands of the metallic surface. The peak at around 400.4 eV (panel d) is also visible as a shoulder of the cyano in-plane resonance in the measured DMC/Cu(001) spectrum for grazing incidence (panel b).

At 404.6 eV, there is a strong σ-shape resonance visible for all spectra of 90° incidence in Figure 7. This resonance is found to result from N 1s → σ^* (azo) transitions. The same resonance for the gas phase molecule (see Figure 4b) turns out to be much weaker in intensity compared to the other spectral features and is located at higher energies than on Cu(001). To ascertain the origin of this peculiarity we calculated the NEXAFS of a DMC molecule by keeping the geometry fixed as for the adsorbate on Cu(001), but in the absence of the metal cluster. This yields the σ-shape resonance at the same energy position as for the adsorbate system. Thus, we can exclude that a direct electronic interaction between the surface and the central molecular σ-bond orbital is responsible for this resonance. Another possible origin is the surface-induced bending of the molecular geometry, which reduces the overlap in the π bonds of the azo group. Together with the attractive forces between the azo nitrogen atoms and Cu(001), this increases the N−N bond distance and reduces the overlap in the N−N σ bond, resulting in a lower splitting between the σ and the σ^* energy levels. It is worth noting the very high sensitivity of the energy position of this σ^* shape resonance on the N−N bond distance with a calculated value of 2 eV/Å.

The resulting picture includes chemisorption of DMC at the surface via the central azo bridge. The formation of a coordination network involving Cu adatoms and the cyano groups, as discussed for 9,10-anthracenedicarbonitrile on Cu(111),[38] is not observed here. While we cannot exclude alternative scenarios in which Cu adatoms are present on the surface and somehow involved in the N−Cu bonds of the azo bridge they are not expected to alter the conclusions extracted from the NEXAFS data significantly.

At this point, we have to remark that we found the DMC molecules at a coverage of 0.4 ML much more flat on the surface than in the case of 0.5 ML. Obviously the stronger lift-up of the benzonitrile moieties out of the surface plane is not only caused by the bond formation to the surface, but it seems to be also influenced by the molecular density in the organic layer.

The corresponding N 1s XPS of 0.4 ML DMC molecules evaporated on Cu(001) at 300 K is given in Figure 9a. The peak assignment of the spectrum is similar to the one of 0.5 ML at room temperature in the temperature-dependent measurement with a dominating signal between 398 and 399 eV (Figure

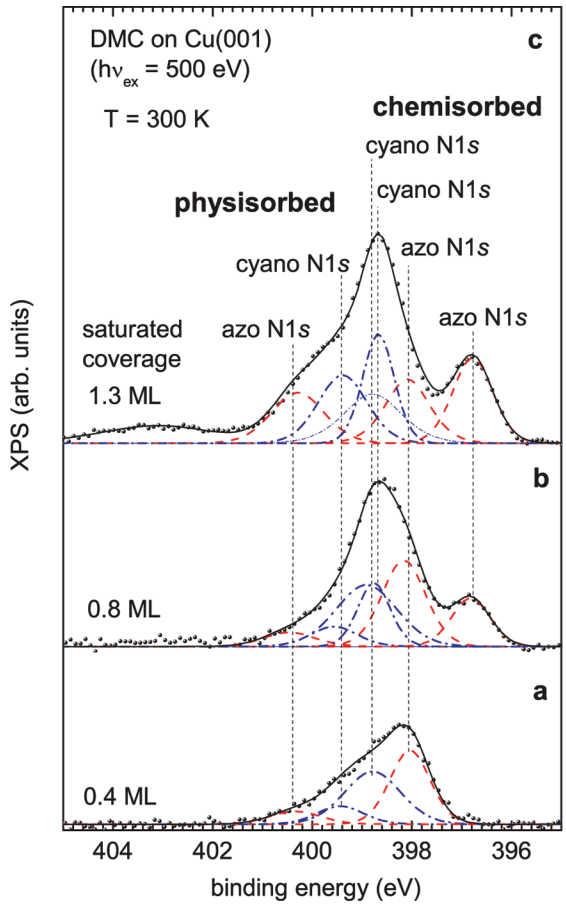

Figure 9. N 1s XPS spectra for increasing coverages of DMC on Cu(001) evaporated at room temperature. The dashed red and the dashed-dotted blue lines are the fitted curves for the azo and cyano excitation centers. Spectra are shifted vertically for clarity.

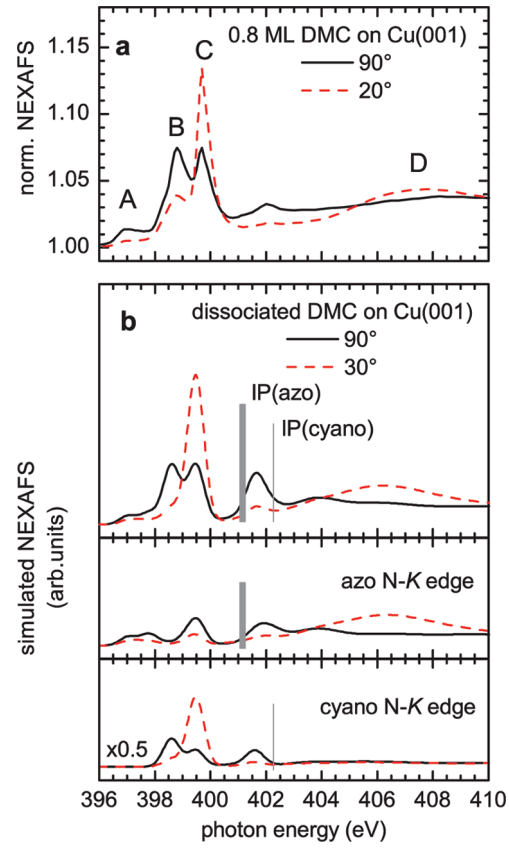

Figure 10. (a) N−K edge NEXAFS measured for 1 ML DMC evaporated on Cu(001) at room temperature. (b) Simulated NEXAFS spectra of dissociated azobenzene on a Cu(001) surface (cf. Figure 11). Gray bars mark the corresponding ionization barriers. The two lower panels in part b show the angle-dependent absorption spectra of the different excitation centers. Continuous lines correspond to spectra acquired or simulated for 90° normal X-ray incidence while dotted lines correspond to the spectra measured under 20° grazing and simulated for 30° grazing X-ray incidence.

5a). For the 0.4 ML DMC evaporated at room temperature the contribution of physisorbed DMC at higher binding energies is smaller, so that the overall spectral shape appears more asymmetric. As a noticeable difference, the spectrum of 0.5 ML exhibits a small shoulder at 397 eV, which may come from an additional species that appears at higher coverage.

Adsorption at High Coverage on Cu(001). Figure 9b,c shows the N 1s XPS of DMC for higher coverages. For 0.8 ML, an additional peak at 397 eV appears at the same energy position as the shoulder in the spectrum of 0.5 ML coverage discussed above. Obviously a new species starts to grow in the presence of the flatly chemisorbed DMC. Consequently, three different pairs of azo and cyano XPS peaks have to be considered in the fitting spectrum, belonging to the small amount of physisorbed DMC and to the two chemisorbed species which appear consecutively with increasing coverage. By a further deposition of DMC up to the saturation coverage the intensity of the peak at 397 eV increases as shown in Figure 9c. At the same time, the amount of physisorbed molecules remains constant. Very likely the additional physisorbed molecules are accumulated into a second layer. The intensity of this species contributes with one-fourth to the entire spectrum. Thus we refer to this coverage as 1.3 ML. For all other samples the coverages are calibrated with respect to this saturated layer.

To characterize the additional chemisorbed species, the corresponding angle-resolved N *K* edge NEXAFS spectra of 0.8 ML DMC on Cu(001) was measured (see Figure 10). Evident differences to the spectra of 0.4 ML DMC on Cu(001) (Figure 7) appear as a new π^*-resonance peak at 397 eV labeled as A, and a shift of the σ-shape resonance at 407.4 eV (feature D) to higher energies. Most strikingly, the angle dependence of the entire spectrum is reversed. The π^* resonance at 399.7 eV (C) as well as the σ-shape resonance are now more pronounced at 20° grazing incidence while the features at around 398.6 eV (B) are more intense in the spectrum of 90° normal incidence. The strong angular dependence suggests that the molecular film remains highly ordered. Since the shape and energy position of peak C at 399.7 eV agree with the ones at 0.4 ML DMC on Cu(001) we can assume the cyano group to be unaffected by any direct interaction with the surface. From the angle dependence of peaks B and C, we conclude that the benzonitrile moieties are more tilted out of the surface plane compared to the molecules in 0.4 ML coverage.

Considering the sp^2 character of the σ-bond backbone of the azo center, the angle between the two azo-phenyl bonds can vary between 60 and 180° by a rotation of the two azobenzene halves around the N≡N bond axis without changing the overlap of the two nitrogen sp^2 orbitals. Assuming furthermore the azo bond axis in the surface plane, the tilt angle θ (see inset in Figure 11) can vary between 30 and 90° without changing the binding energy of the azo σ bond. Further bending of the benzonitrile moieties toward the surface normal will reduce the overlap of the two nitrogen sp^2 orbitals, weakening the N═N double bond, and may eventually lead to dissociation of the azo center. To

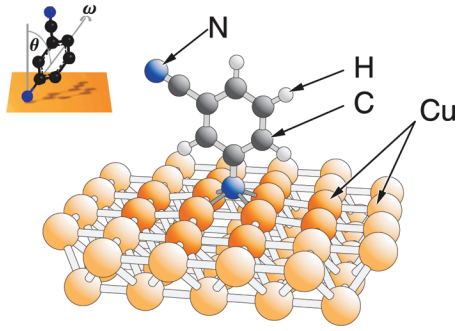

Figure 11. Relaxed geometric structure of a single dissociated DMC azobenzene subunit on top of a Cu_{57} cluster, resulting from DFT geometry optimization. Darker and brighter substrate atoms were free and fixed during optimization, respectively. In the inset, the two angles θ and ω are defined to uniquely describe the orientation of the benzonitrile moiety with respect to the surface normal.

substantiate this issue, we performed DFT calculations of a dissociated DMC subunit on Cu(001), as presented in Figure 11. The geometry optimization shows that the molecule adsorbs via the azo nitrogen in a hollow Cu(001) site perpendicular to the surface. The very good agreement of the simulated NEXAFS spectra, shown in Figure 10b, with the experimental data in Figure 10a supports the suggested dissociation process. The low-energy π^* resonance (peak A) corresponds to an additional N−Cu(001) bond oriented in the surface plane. The angle dependence of the σ-shape resonance (peak D) proves the absence of an azo σ bond lying in the surface plane. The only discrepancy between the experimental and simulated data appears in peak B at grazing incidence. This intensity is explained by the presence of a second species of intact chemisorbed DMC, as observed for 0.4 ML coverage, which will contribute only to the grazing spectrum at the energy of peak B. Since we can assume the two π^* orbitals of the cyano triple bond, corresponding to the resonances at 398.6 and 399.7 eV, to be perpendicular with respect to each other (cf. LUMO+1 and LUMO+2 in Figure 3), it is possible to use their angle dependencies[12,37] to calculate the tilt angle θ of the dissociated DMC subunits as well as the rotation angle ω defined in Figure 11. The angle dependence of the difference spectra referring only to the dissociated species yields $\theta = 8°$ and $\omega = 75°$. In contrast, the values derived from the geometry optimization are $\theta = 0°$ with ω arbitrary. The difference between experiment and theory can be explained by the influence of intermolecular interactions which are not considered in the DFT calculation.

Conclusions

In this paper, we have studied the adsorption of CMA and DMC azobenzene molecules at metallic surfaces by means of XPS and angle dependent NEXAFS measurements comparing the results to DFT simulations. Au(111) and Cu(001) are used as substrates with different bond strengths. In the case of Au(111) at room temperature, 1 ML DMC is physisorbed lying flat on the surface in the trans conformation with an electronic structure similar to that calculated for the free molecule. In contrast, on Cu(001) a mixture of physisorbed and chemisorbed species appears already at low substrate temperatures of 150 K. During annealing the sample to room temperature almost all physisorbed molecules pass into the chemisorbed state above 250 K. The chemisorbed DMC species is characterized by the substitution of the central azo π bond with covalent bonds to the Cu(001) substrate. As a result, the benzonitrile moieties are tilted out of the surface plane. The influence of the molecule−substrate and intermolecular interactions was studied separately by comparing experimental NEXAFS data with simulated results from DFT calculations. We conclude that the chemisorbed DMC molecules exhibit a strongly distorted geometry with an increased bond length of the azo N═N bond due to the presence of the Cu(001) surface. By increasing the coverage to 1 ML DMC on Cu(001), the intermolecular interactions lead to the dissociation of the additional azobenzene molecules at the azo center, so that the benzonitrile moieties are almost perpendicular to the surface plane.

Acknowledgment. This work is supported by the DFG (Sfb 658 TP B3). We thank B. Zada and W. Mahler for their technical support during the measurements at BESSY.

References and Notes

(1) Kausar, A.; Nagano, H.; Ogata, T.; Nonaka, T.; Kurihara, S. *Angew. Chem., Int. Ed.* **2009**, *48*, 2144.
(2) Sadovski, O.; Beharry, A. A.; Zhang, F.; Woolley, G. A. *Angew. Chem., Int. Ed.* **2009**, *48*, 1484.
(3) Lim, H. S.; Han, J. T.; Kwak, D.; Jin, M.; Cho, K. *J. Am. Chem. Soc.* **2006**, *128*, 14458.
(4) Wang, Y.; Ge, X.; Schull, G.; Berndt, R.; Bornholdt, C.; Koehler, F.; Herges, R. *J. Am. Chem. Soc.* **2008**, *130*, 4218.
(5) Henningsen, N; Franke, K. J.; Torrente, I. F.; Schulze, G.; Priewisch, B.; Rück-Braun, K.; Dokic, J.; Klamroth, T.; Saalfrank, P.; Pascual, J. I. *J. Phys. Chem. C* **2007**, *111*, 14843.
(6) Henningsen, N.; Rurali, R.; Franke, K. J.; Fern, I.; Pascual, J. I. *Appl. Phys. A* **2008**, *93*, 241.
(7) Piantek, M.; Miguel, J.; Bernien, M.; Navío, C.; Krüger, A.; Priewisch, B.; Rück-Braun, K.; Kuch, W. *Appl. Phys. A* **2008**, *93*, 261.
(8) Lei, Z.; Vaidyalingam, A.; Dutta, P. K. *J. Phys. Chem. B* **1998**, *102*, 8557.
(9) Henzl, J.; Mehlhorn, M.; Morgenstern, K. *Nanotechnology* **2007**, *18*, 495502.
(10) Comstock, M. J.; Cho, J.; Kirakosian, A.; Crommie, M. F. *Phys. Rev. B* **2005**, *72*, 153414.
(11) Comstock, M. J.; Levy, N.; Kirakosian, A.; Cho, J.; Lauterwasser, F.; Harvey, J. H.; Strubbe, D. A.; Frechet, J. M. J.; Trauner, D.; Louie, S. G.; Crommie, M. F. *Phys. Rev. Lett.* **2007**, *99*, 038301.
(12) Ballav, N.; Schupbach, B.; Dethloff, O.; Feulner, P.; Terfort, A.; Zharnikov, M. *J. Am. Chem. Soc.* **2007**, *129*, 15416.
(13) Hermann, K.; Pettersson, L. G. M. *StoBe program package*; Stockholm, Berlin, 2005, (A modified version of the DFT-LCGTO program package deMon; A. St.-Amant, A.; Salahub, D., University of Montreal).
(14) Perdew, J. P.; Burke, K.; Ernzerhof, M. *Phys. Rev. Lett.* **1996**, *77*, 3865.
(15) Hammer, B.; Hansen, L. B.; Nørskov, J. K. *Phys. Rev. B* **1991**, *59*, 7413.
(16) Godbout, N.; Salahub, D. R.; Andzelm, J.; Wimmer, E. *Can. J. Chem.* **1992**, *70*, 560.
(17) Kutzelnigg, W.; Fleischer, U.; Schindler, M. *NMR-Basic Principles and Progress*; Springer: Heidelberg, 1990; Vol. 23, p 165.
(18) Mattsson, A.; Panas, I.; Siegbahn, P.; Wahlgren, U.; Akeby, H. *Phys. Rev. B* **1987**, *36*, 7389.
(19) Ågren, H.; Carravetta, V.; Vahtras, O.; Pettersson, L. G. M. *Theor. Chem. Acc.* **1997**, *97*, 14.
(20) Fliegl, H.; Kohn, A.; Hattig, C.; Ahlrichs, R. *J. Am. Chem. Soc.* **2003**, *125*, 9821.
(21) Rurali, R.; Pascual, J. I. private communication
(22) Slater, J. C. In *Advances in Quantum Chemistry*; Loewdin, P. O., Ed.; Academic: New York, 1972; p 1.
(23) Slater, J. C.; Johnson, K. H. *Phys. Rev. B* **1972**, *5*, 844.
(24) Hermann, K. In *Computational Methods in Catalysis and Material Science*; Wiley-VCH: Weinheim, 2009; p 375.
(25) Leetmaa, M.; Ljundberg, M.; Nilson, A.; Pettersson, L. G. M. *Computational Methods in Catalysis and Material Science*; Wiley-VCH: Weinheim, 2009; p 221.
(26) Dimitrova, Y. *J. Mol. Struct.* **1996**, *362*, 23.
(27) Kagiya, T.; Sumida, Y.; Inoue, T. *Bull. Chem. Soc. Jpn.* **1968**, *41*, 767.
(28) Ohta, T.; Fujikawa, T.; Kuroda, J. *Bull. Chem. Soc. Jpn.* **1975**, *48*, 2017.
(29) Füchsel, G. F.; Klamroth, T.; Dokic, J.; Saalfrank, P. *J. Phys. Chem. B* **2006**, *110*, 16337.

(30) Rangan, S.; Gallet, J.-J.; Bournel, F.; Kubsky, S.; Le Guen, K.; Dufour, G.; Rochet, F.; Sirotti, F.; Carniato, S.; Ilakovac, V. *Phys. Rev. B* **2005**, *71*, 165318.

(31) Carniato, S.; Ilakovac, V.; Gallet, J.-J.; Kukk, E.; Luo, Y. *Phys. Rev. A* **2005**, *71*, 022511.

(32) Cavalleri, M.; Hermann, K.; Guimond, S.; Romanyshyn, Y.; Kuhlenbeck, H.; Freund, H.-J. *Catal. Today* **2007**, *124*, 21.

(33) Kolczewski, C.; Williams, F. J.; Cropley, R. L.; Vaughan, O. P. H.; Urquhart, A. J.; Tikhov, M. S.; Lambert, R. M.; Hermann, K. *J. Chem. Phys.* **2006**, *125*, 034701.

(34) Menzel, D. *Crit. Rev. Solid State Mater. Sci.* **1978**, *7*, 357.

(35) Nakayama, T.; Inamura, K.; Inoue, Y.; Ikeda, S. *Surf. Sci.* **1987**, *179*, 47.

(36) Stöhr, J. *NEXAFS Spectroscopy*; Springer: Berlin, 1992; p 172 ff.

(37) Stöhr, J. *NEXAFS Spectroscopy*; Springer; Berlin, 1992; p 276 ff.

(38) Pawin, G.; Wong, K. L.; Kim, D.; Sun, D.; Bartels, L.; Hong, S.; Rahman, T. S.; Carp, R.; Marsella, M. *Angew. Chem.* **2008**, *120*, 8570.

JP907641F